analytical chemistry

Letter

pubs.acs.org/ac

Hapten-Grafted Graphene as a Transducer for Homogeneous Competitive Immunoassay of Small Molecules

Feng Long,*[,†] Anna Zhu,[‡] Hanchang Shi,[§] and Hongchen Wang[†]

[†]School of Environment and Natural Resources, Renmin University of China, Haidian, Beijing 100872, China

[‡]Department of Chemistry, Massachusetts Institute of Technology, Cambridge, MA 02139, United States

[§]State Key Joint Laboratory of ESPC, School of Evironment, Tsinghua University, Beijing 100084, China

Supporting Information

ABSTRACT: A hapten-grafted graphene-based biosensor by integrating both the graphene nanosheets and immunoassay sensing technologies was developed for ultrasensitive homogeneous competitive immunoassay of small molecules. The structure of hapten-grafted graphene avoids the activity loss of biomolecules immobilized onto the graphene surface and is beneficial to preserve the binding affinity between small molecule and its specific antibody. The sandwich structure formed between hapten-grafted graphene nanosheets and fluorescence-labeled antibody increases the quenching efficiency of the organic dye, thereby resulting in high signal-to-background ratios and improved sensitivity for Bisphenol A (BPA) detection. On the basis of fluorescence resonance energy transfer (FRET) and homogeneous competitive immunoassay mechanism, high BPA concentrations in the sample reduce the amount of fluorescence-labeled anti-BPA antibody bound to graphene-BPA nanosheets, thus resulting in remarkable fluorescence signals. The linear quantification of BPA over concentration ranges from 0.5 to 50 nM with a detection limit determined as 0.12 nM. These findings show that the proposed method provides a powerful tool for the rapid and sensitive detection of small molecules in biological and environmental samples.

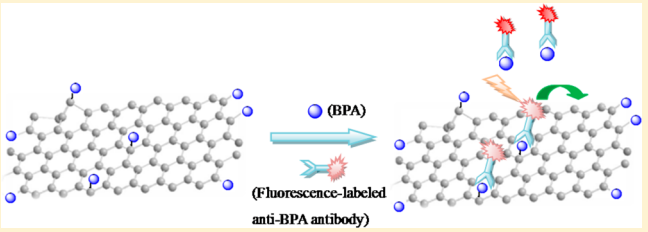

Nanobiosensors with their excellent nanoscale properties have gained considerable interest for their use in the rapid and sensitive detection of small molecules;[1−3] such capability is essential in clinical diagnostics,[1−5] food analysis,[6] and environmental monitoring.[7−9] Because of their excellent electrical, optical, mechanical, and transport properties, two-dimensional graphene-based materials functionalized with biomolecules (e.g., antibodies and DNA) have emerged as potential transducers in diverse analytical devices.[1,4,8−11] However, experiments[12,13] and simulations[14,15] show significant conformational changes and loss of function of the biomolecules adsorbed or covalently linked to the nanomaterial surface,[16,17] the activity and selectivity of which rely on a specific tertiary or quaternary structure. Upon conjugation of graphene with an antibody, the binding site is disrupted, resulting in the degradation of antibody performance and reductions in sensor sensitivity.[16,17] Controlling the orientation and position of the antibody relative to graphene remains a great challenge to many scientists.[11,17]

We report a facile and robust fluoroimmunosensor using hapten-grafted graphene nanosheets for the rapid and sensitive detection of small molecules. In this nanosensor, hapten-grafted graphene nanosheets regarded as the immunological recognition of fluorescence-labeled antibody as well as for optical transduction, which can avoid the above-mentioned drawbacks. On the basis of either the photoinduced electron transfer mechanism or the energy transfer mechanism, graphene is employed as an efficient fluorescence quencher for the development of fluorescence resonance energy transfer (FRET) biosensors because of its excellent quenching capability toward various organic dyes and quantum dots.[2,9,11] Figure 1 shows a graphene-based FRET platform. Bisphenol A (BPA), a xenoestrogenic endocrine-disrupting chemical widely detected in the environment and food, was selected as a model target. BPA causes cardiovascular disease, diabetes, neurobehavioral disorders, carcinogenic hypersensitivity, and reproductive impairment.[7,18] 4,4 Bis-(4-hidroxyphenyl) valeric acid (BVA), a structural analog of BPA with a carboxyl group, was conjugated to aminated graphene through carbodiimide-assisted amidation with EDC and NHS (Figure S1 of the Supporting Information). Figure 1 illustrates the competitive immunoassay mechanism for BPA detection. High BPA concentrations in the sample reduce the amount of fluorescence-labeled antibody bound to graphene-BPA nanosheets, which causes remarkable fluorescence signals. BPA can then be detected sensitively and quantitatively.

RESULTS AND DISCUSSION

Figure S2 of the Supporting Information shows the Raman spectra of aminated and BPA-grafted graphene. The G-band

Received: January 27, 2014
Accepted: March 3, 2014
Published: March 3, 2014

   dx.doi.org/10.1021/ac500347n | *Anal. Chem.* 2014, 86, 2862−2866

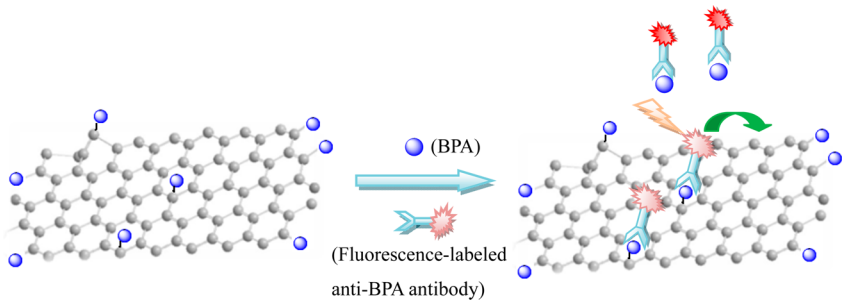

Figure 1. Schematic illustration of the homogeneous competitive immunoassay for BPA in water samples.

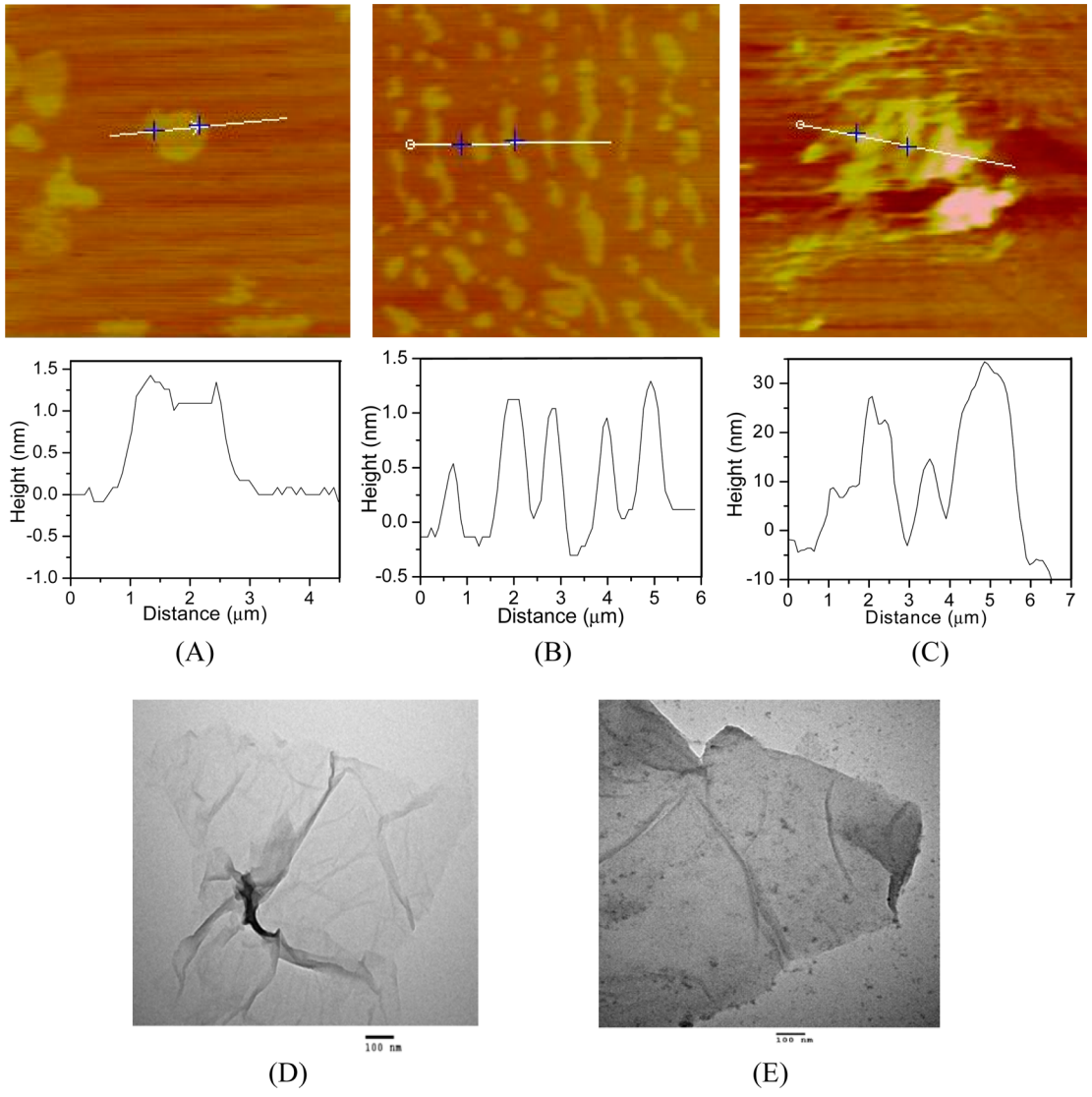

Figure 2. (A–C) AFM images and height profiles of aminated graphene, graphene-BPA conjugate, and anti-BPA antibody-conjugated graphene on freshly cleaved mica. The antibody-conjugated graphene nanosheets exhibited brighter spots with increased heights on their surfaces. (D–E) TEM images of aminated graphene and antibody-conjugated graphene.

position of BPA-grafted graphene shifted to lower frequency by ~4 cm^{-1} compared with that of aminated graphene (1590 cm^{-1}). This phenomenon is attributed to the strong bond formed by chemical grafting of graphene and the attached molecules, which affects its electronic structure of the resultant product.[19] A similar result has been reported for covalently functionalized graphene.[20] The integrated intensity ratio of the D and G peaks (I_D/I_G) of graphene-NH_2 is 0.95, while that of BPA-grafted graphene is 1.05, which corresponds to an increase of 10.5%. The I_D/I_G ratio reveals the extent of defects in modified graphene surface and characterizes the degree of covalent functionalization.[19−21] The slightly increased value observed may be attributed to the formation of covalent bonds between aminated graphene and BPA by the well-established carbodiimide reaction,[20] rather than further damage to the graphene surface structure, similar to previously described

dx.doi.org/10.1021/ac500347n | *Anal. Chem.* 2014, 86, 2862−2866

covalent functionalizations of graphene.[19,20] Fourier transform-infrared (FT-IR) spectroscopy also confirms the successful grafting of BPA molecules onto the surface of the aminated graphene nanosheets (Figure S3 of the Supporting Information).

Figure 2A shows an AFM image of the aminated graphene as well as the representative height profiles. The latter reveals that the aminated graphene nanosheets are 1.2 nm thick, thereby confirming the monolayer structure of the nanomaterials. Figure 2B shows an AFM image of graphene-BPA as well as its representative height. No obvious difference compared with the height profile of aminated graphene was observed, likely because of the small size of BPA. Following grafting of aminated graphene with BPA, a graphene-BPA conjugate with good monodispersity was obtained. Addition of anti-BPA antibody to the graphene-BPA solution resulted in graphene-BPA bound with anti-BPA antibody and agglomeration assembly of molecules. The antibody-linked graphene shows brighter spots (Figure 2C). With consideration of the theoretical value of an antibody (6−10 nm)[22,23] and graphene (1.2 nm), measured heights of over 25−30 nm showed that the assembly between the antibody and graphene-BPA nanosheets forms a bilayer or multilayer structure. These results were further confirmed by transmission electron microscopy (TEM). The morphologies of functionalized graphene-BPA nanosheets and graphene-BPA/anti-BPA antibody conjugate are shown in Figure 2 (panels E and F). In the absence of the antibody, the graphene-BPA yielded a very clear and monolayer structure (Figure 2D). However, anti-BPA antibody bound to graphene-BPA and a multilayer graphene structure were formed upon addition of anti-BPA antibody (Figure 2E). We assumed that the sandwich structure of graphene/antibody/graphene is formed when an antibody is added to the graphene-BPA solution because each antibody has two binding sites that can simultaneously bind with two BPA molecules. This antibody/graphene/antibody structure can also occur because graphene is a two-dimensional nanomaterial, and graphene-BPA can bind with antibodies in various orientations.

To reduce the effect of nonspecific adsorption of antibodies on the graphene surface, 2 mg/mL BSA, which can effectively block the nonspecific adsorption sites of graphene,[24] was added to the mixture of fluorescence-labeled antibody and graphene-BPA nanosheets (Figure S4 of the Supporting Information). Several control experiments confirmed that fluorescence quenching contributed to the FRET between graphene-BPA nanosheets and fluorescence-labeled anti-BPA antibody (Figure S5 of the Supporting Information). We analyzed the emission spectra of fluorescence-labeled anti-BPA antibody as a function of graphene-BPA nanosheet concentration to further confirm quenching efficiency of this system. Figure S5 of the Supporting Information shows that the fluorescence intensities of fluorescence-labeled antibody (fixed concentration of 0.3 μg/mL) gradually decreases as the graphene-BPA concentration increases from 0.0 to 12.0 μg/mL and that the maximum quenching may be observed in 12.0 μg/mL graphene-BPA nanosheets. The quenching efficiency was calculated using the formula $1 - I/I_0$, where I_0 and I represent the fluorescence intensities of fluorescence-labeled anti-BPA antibody in the absence and presence, respectively, of the graphene-BPA nanosheets. A maximum quenching efficiency of up to 90.4% was obtained when 12.0 μg/mL graphene-BPA nanosheets was utilized (Figure S6 of the Supporting Information). The fluorescence quenching efficiency of the fluorescence-labeled anti-BPA antibody in this system was inversely proportional to the graphene-BPA concentration when the concentration of graphene-BPA was less than 2.0 μg/mL. To further increasing the concentration of graphene-BPA, the quenching efficiency of the system slowly increases and then plateaus.

In this fluorescence-labeled anti-BPA antibody/graphene-BPA system, the quenching mechanisms are assumed to contribute to the following reasons. First, FRET is generally most efficient when the distance between donors and acceptors is between 20 and 60 Å.[25] Because the size of BPA is very small, the distance between graphene and the dye labeled on the antibody may contribute to the size of antibody, which is about 6−10 nm.[22,23] With consideration that the graphene-BPA ensemble likely displays a heterogeneous mixture of multiple hapten orientations and binding sites, the fluorescence-labeled antibody easily binds to the graphene in various random orientations. Furthermore, the sandwich structure of the graphene-BPA nanosheet and fluorescence-labeled anti-BPA antibody assembly causes some dyes to come into close proximity with the graphene surface, which maximizes the quenching efficiency of the system. Second, theoretical calculations indicated that graphene could act as a universal and highly efficient long-range quencher because of its electronic properties, similarities, and dissimilarities with metal surfaces.[26,27] The rate of long-range resonance energy transfer is suggested to have a $(\text{distance})^{-4}$ dependence, and quenching could be observable up to a distance of about 300 Å. Third, spectral overlap between the emission of the donor and the absorbance of the acceptor is generally required for FRET to occur.[28] Kim et al. previously demonstrated that with using graphene as an acceptor, the FRET effect is independent of the emission spectra of the donor and reduced graphene oxide (GO) shows a better performance than GO as a quencher when organic dyes are used as donors.[29] Fourth, the large surface area of graphene corresponds to an increased number of FRET acceptor molecules.[30] With the increased number of acceptor molecules, the fraction of photons absorbed by donors that are transferred to acceptors is generally increased in a FRET system.[31] In addition, the two-dimensional structure of the graphene-BPA nanosheets inhibits steric hindrance, and improves the binding reaction between the antigen and the antibody.

To determine the optimum concentration of graphene-BPA nanosheets and fluorescence-labeled anti-BPA antibodies, a sensitivity index (ε) was introduced:

$$\varepsilon = \frac{I_0 - I_s}{I_0 - I_b} \quad (1)$$

where I_b is the fluorescence intensity of the mixture of fluorescence-labeled anti-BPA antibody and graphene-BPA nanosheets and I_s is the fluorescence intensity of the mixture of fluorescence-labeled anti-BPA antibody and graphene-BPA nanosheets after addition of 10 nM BPA. Checkerboard titration was performed with serial dilution of fluorescence-labeled anti-BPA antibody and graphene-BPA nanosheets for various combinations (Figure S7 of the Supporting Information). For a certain concentration of fluorescence-labeled anti-BPA antibody, the higher is the concentration of graphene-BPA nanosheets, the larger is the extent of binding and quenching of fluorescence-labeled anti-BPA antibody on the graphene surface, leading to lower fluorescence signals. For a certain concentration of graphene-BPA nanosheets, increasing the

dx.doi.org/10.1021/ac500347n | Anal. Chem. 2014, 86, 2862−2866

fluorescence-labeled anti-BPA antibody concentration obviously resulted in an increase in fluorescence signals. Figure S8 of the Supporting Information demonstrates the fluorescence quenching efficiency observed at different concentrations of graphene-BPA and fluorescence-labeled anti-BPA antibody. The sensitivity index also calculated from the fluorescence intensity in the presence of BPA and in the absence of the target antigen (Figure S8 of the Supporting Information). Considering the signal intensity level required and a reasonable dynamic detection range, the sensitivity index should be as low as possible (preferably below than 0.9) and the fluorescence quenching efficiency should be as high as possible (favorably larger than 0.8). Therefore, 3 μg/mL graphene-BPA nanosheets and 10 nM fluorescence-labeled anti-BPA antibody were chosen as the optimum pair of sensing elements for subsequent BPA measurements.

On the basis of the results obtained above, we applied a graphene-based FRET nanosensing platform to detect BPA using a homogeneous competitive immunoassay mechanism. Standard BPA solutions of various concentrations and graphene-BPA of a fixed concentration were initially mixed. Fluorescence labeled anti-BPA antibody of a specific concentration was then added to this mixture, which was subsequently incubated for 5 min. During incubation, the amount of BPA in the sample was expected to compete with BPA covalently immobilized onto the graphene surface to bind with the limited binding sites of the anti-BPA antibody, thereby producing a target concentration-dependent fluorescence signal, which is the basis of quantitative detection. Figure 3A shows the fluorescence spectra of the graphene-BPA/fluorescence-labeled anti-BPA antibody FRET system obtained with varying concentrations of BPA. The fluorescence intensity of the system increased gradually with BPA concentrations ranging from 0 to 100 nM. The fluorescence-enhanced efficiency was calculated as

$$E = \frac{I_s - I_b}{I_0 - I_b} \quad (2)$$

Figure 3B shows a calibration plot of the fluorescence-enhanced efficiency as a function of the BPA concentration. The fluorescence-enhanced efficiency exhibited a linear trend with BPA concentrations between 0.5 and 50 nM (correlation coefficient of 0.9936), and the calibration curve was expressed as $E = 0.2219 + 0.4386c$ (where c is in nanomolar). The limit of detection (defined as 3σ/slope) for BPA was 0.12 nM. This sensitivity is also either better or favorably comparable with those of previous nanosensors, reviewed by Ragavan et al.[7] Such high sensitivity is attributed to the high binding ability of the antibody−antigen and the excellent quenching behavior of graphene.

To evaluate the feasibility of the developed sensor in actual detection, the biosensor was applied to determine BPA levels in several water samples (e.g., tap water, lake water, and bottled water). The developed assay showed the recoveries ranging from 85% to 115% for the water samples and a relative standard deviation of around 7.9% (Table S1 of the Supporting Information). These results confirm that the developed sensor is highly reproducible and can be applied in the detection of BPA in real water samples.

In summary, a graphene-hapten-based FRET system provides a general and promising platform for the immunoassay of small molecules by taking advantage of the unique

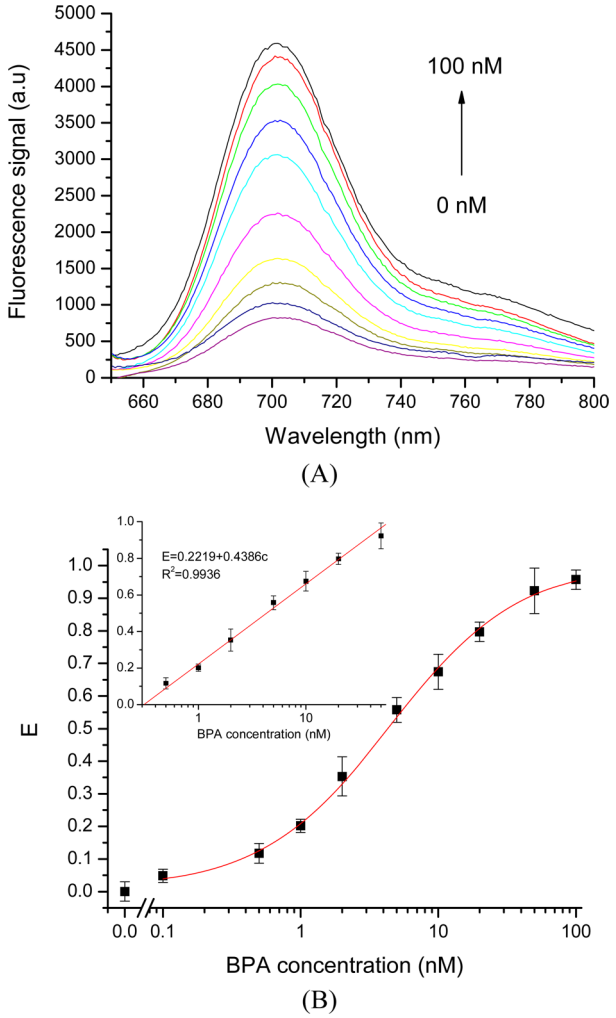

Figure 3. (A) Fluorescence spectra of the fluorescence-labeled anti-BPA antibody/graphene-BPA system in the presence of different concentrations of BPA in 0.01 M phosphate buffer (pH 7.10). From bottom to top: 0, 0.1, 0.5, 1, 2, 5, 10, 20, 50, and 100 nM BPA. Fluorescence-labeled anti-BPA antibody, 10 nM; graphene-BPA, 3 μg/mL. (B) Fluorescence-enhanced efficiency as a function of BPA concentration. Inset: Linear relationship between the BPA concentration and fluorescence-enhanced efficiency.

interactions between hapten-grafted graphene and fluorescence-labeled antibody as well as the excellent quenching efficiency of graphene. The proposed approach possessed several features and advantages: first, the structure of graphene-hapten avoids the loss of activity observed in biomolecules immobilized onto graphene surfaces, which allows much better antibody−antigen binding and rapid on-site analysis of small molecules. Second, the sandwich structure formed between hapten-grafted graphene nanosheets and fluorescence-labeled antibody increases the quenching efficiency of the organic dye, thereby providing low background signals and slight background fluctuation. These characteristics result in high signal-to-background ratios and improved sensitivity for BPA detection. Third, the proposed method may be extended to the detection of other analytes by modifying other haptens to functional graphene (e.g., aminated or carboxylation graphene). Furthermore, because small molecules can be recognized by other biofunctional molecules (e.g., MIPs, aptamers, receptors),

dx.doi.org/10.1021/ac500347n | Anal. Chem. 2014, 86, 2862−2866

we expected that the general approach presented in this work will facilitate the design and development of other biosensors.

■ ASSOCIATED CONTENT

Supporting Information

Additional information as noted in text. This material is available free of charge via the Internet at http://pubs.acs.org.

■ AUTHOR INFORMATION

Corresponding Author

*E-mail: longf04@mails.thu.edu.cn.

Notes

The authors declare no competing financial interest.

■ ACKNOWLEDGMENTS

This research was financially supported by the National Natural Science Foundation of China (Grants 21077063 and 21277173), the National Instrument Major Project of China (Grant 2012YQ3011105), and the Basic Research funds in Renmin University of China from the central government (Grant 13XNLJ01).

■ REFERENCES

(1) Wang, J.; Qu, X. *Nanoscale* **2013**, *5*, 3589−3600.
(2) Kim, N. H.; Lee, J. H.; Liu, Y.; Dong, X.; Chen, P. *Chem. Soc. Rev.* **2012**, *41*, 2283−2307.
(3) Patolsky, F.; Zheng, G. F.; Lieber, C. M. *Nat. Protoc.* **2006**, *1*, 1711−1724.
(4) Huang, X.; Qi, X. Y.; Boey, F.; Zhang, H. *Chem. Soc. Rev.* **2012**, *41*, 666−686.
(5) Wang, W. U.; Chen, C.; Lin, K. H.; Fang, Y.; Lieber, C. M. *Proc. Natl. Acad. Sci. U.S.A.* **2005**, *102*, 3208−3212.
(6) Farahi, R. H.; Passian, A.; Tetard, L.; Thundat, T. *ACS Nano* **2012**, *6*, 4548−4556.
(7) Ragavan, K. V.; Rastogi, N. K.; Thakur, M. S. *Trends Anal. Chem.* **2013**, *52*, 248−260.
(8) Zhou, X. H.; Liu, L. H.; Bai, X.; Shi, H. C. *Sens. Actuators, B* **2013**, *181*, 661−667.
(9) Shi, Y.; Wu, J.; Sun, Y.; Zhang, Y.; Wen, Z.; Dai, H.; Wang, H.; Li, Z. *Biosens. Bioelectron.* **2012**, *38*, 31−36.
(10) Lee, J. S.; Joung, H.; Kim, M.; Park, C. B. *ACS Nano* **2012**, *6*, 2978−2983.
(11) Jung, J. H.; Cheon, D. S.; Liu, F.; Lee, K. B.; Seo, T. S. *Angew. Chem., Int. Ed.* **2010**, *49*, 5708−5711.
(12) De, M.; Chou, S. S.; Dravid, V. P. *J. Am. Chem. Soc.* **2011**, *133*, 17524−17527.
(13) Katoch, J.; Kim, S. N.; Kuang, Z.; Farmer, B. L.; Naik, R. R.; Tatulian, S. A.; Ishigami, M. *Nano Lett.* **2012**, *12*, 2342−2346.
(14) Zuo, G.; Zhou, X.; Huang, Q.; Fang, H.; Zhou, R. *J. Phys. Chem. C* **2011**, *115*, 23323−23328.
(15) Ou, L.; Luo, Y.; Wei, G. *J. Phys. Chem. B* **2011**, *115*, 9813−9822.
(16) Alava, T.; Mann, J. A.; Theodore, C.; Benitez, J. J.; Dichtel, W. R.; Parpia, J. M.; Craighead, H. G. *Anal. Chem.* **2013**, *85*, 2754−2759.
(17) Mann, J. A.; Alava, T.; Craighead, H. G.; Dichtel, W. R. *Angew. Chem., Int. Ed.* **2013**, *52*, 3177−3180.
(18) Cabaton, N. J.; Wadia, P. R.; Rubin, B. S.; Zalko, D.; Schaeberle, C. M.; Askenase, M. H.; Gadbois, J. L.; Tharp, A. P.; Whitt, G. S.; Sonnenschein, C.; Soto, A. M. *Environ. Health Perspect.* **2011**, *119*, 547−552.
(19) Hsiao, M. C.; Liao, S. H.; Yen, M. Y.; Liu, P.; Pu, N. W.; Wang, C. A.; Ma, C. M. *Appl. Mater. Interfaces* **2010**, *2*, 3092−2099.
(20) Fang, M.; Wang, K.; Lu, H.; Yang, Y.; Nutt, S. *J. Mater. Chem.* **2009**, *19*, 7098−7105.
(21) Sharma, R.; Baik, J. H.; Perera, C. J.; Strano, M. S. *Nano Lett.* **2010**, *10*, 398−405.
(22) Murphy, R. M.; Slayter, H.; Schurtenberger, P.; Chamberlin, R. A.; Colton, C. K.; Yarmush, M. L. *Biophys. J.* **1988**, *54*, 45−56.
(23) Yarmush, D. M.; Murphy, R. M.; Colton, C. K.; Fisch, M.; Yarmush, M. L. *Mol. Immunol.* **1988**, *25*, 17−25.
(24) Mao, S.; Lu, G. H.; Yu, K. H.; Bo, Z.; Chen, J. H. *Adv. Mater.* **2010**, *22*, 3521−3526.
(25) Lakowicz, J. R. *Principles of Fluorescence Spectroscopy*, 2nd ed.; Kluwer Academic: New York, 1999.
(26) Swathi, R. S.; Sebastian, K. L. *J. Chem. Phys.* **2009**, *130*, 086101.
(27) Huang, P. J. J.; Liu, J. *Small* **2012**, *8*, 977−983.
(28) Sapsford, K. E.; Berti, L.; Medintz, I. L. *Angew. Chem., Int. Ed.* **2006**, *45*, 4562−4589.
(29) Kim, J.; Cote, L. J.; Kim, F.; Huang, J. *J. Am. Chem. Soc.* **2010**, *132*, 8180−8186.
(30) Stankovich, S.; Dikin, D. A.; Dommett, G. H. B.; Kohlhaas, K. M.; Zimney, E. J.; Stach, E. A.; Piner, R. D.; Nguyen, S. T.; Ruoff, R. S. *Nature* **2006**, *442*, 282−285.
(31) Somers, R. C.; Bawendi, M. G.; Nocera, D. G. *Chem. Soc. Rev.* **2007**, *36*, 579.